Formation of C_s-$Ir_3(CO)_3(\eta^5\text{-}C_9H_7)_3$. Interconversion of C_s and C_{3v} Isomers

Matthew C. Comstock and John R. Shapley*

School of Chemical Sciences, University of Illinois, Urbana, Illinois 61801

Received October 17, 2002

The cluster $Ir_3(CO)_3(\eta^5\text{-}C_9H_7)_3$ (**1**) reacts with $HBF_4\cdot Et_2O$ to form $[Ir_3(\mu\text{-}H)(CO)_3(\eta^5\text{-}C_9H_7)_3][BF_4]$ (**2**). Deprotonation of **2** with NEt_3 generates C_s-$Ir_3(CO)_3(\eta^5\text{-}C_9H_7)_3$ (**1c**), which rapidly reverts to an equilibrium mixture containing C_{3v}-$Ir_3(\mu\text{-}CO)_3(\eta^5\text{-}C_9H_7)_3$ (**1a**) as the major isomer. Activation parameters for the reversion are $\Delta H^{\ddagger} = 17.0(3)$ kcal mol^{-1} and $\Delta S^{\ddagger} = -13(1)$ cal mol^{-1} K^{-1}, and $K_{eq} = [\mathbf{1a}]/[\mathbf{1c}] = 16.7(7)$ at 25 °C. Variable-temperature NMR experiments indicate that **1c** undergoes a dynamic process, with $T_c = -30$ °C and $\Delta G_c^{\ddagger} = 12.4(3)$ kcal mol^{-1}, which equilibrates the three indenyl ligands but does not equilibrate the two sets of CO ligands on opposite sides of the Ir_3 plane.

Introduction

As depicted in Chart 1, several structures (A−D) have been observed for trinuclear compounds of the cobalt triad having the general formula $M_3(CO)_3(\eta^5\text{-}L)_3$, where L refers to η^5-C_5H_5 and related ligands.[1−4] We have described the synthesis and characterization of $Ir_3(\mu\text{-}CO)_3(\eta^5\text{-}C_9H_7)_3$ (**1**), with a crystal structure of type A.[5] We now report that the reaction of **1** with $HBF_4\cdot Et_2O$ results in formation of $[Ir_3(\mu\text{−}H)(CO)_3(\eta^5\text{-}C_9H_7)_3][BF_4]$ (**2**) and that subsequent deprotonation provides C_s-$Ir_3(CO)_3(\eta^5\text{-}C_9H_7)_3$ (**1c**), with a solution structure of type C. This isomer is unstable at room temperature and reverts to an equilibrium mixture dominated by C_{3v}-$Ir_3(\mu\text{-}CO)_3(\eta^5\text{-}C_9H_7)_3$ (**1a**). NMR data have been obtained to characterize the stereodynamics of **1c** in solution. Furthermore, kinetic and thermodynamic parameters have been determined for the conversion of **1c** to the equilibrium mixture **1a/1c**. This system represents a unique example of facile interconversion between structural isomers of type C and type A.

Chart 1

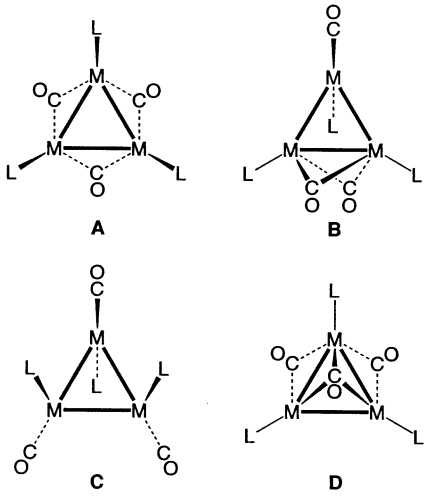

Results and Discussion

Protonation of $Ir_3(CO)_3(\eta^5\text{-}C_9H_7)_3$. Addition of 1 equiv of $HBF_4\cdot Et_2O$ to a red solution of **1** in dichloromethane results in immediate formation of a purple solution, which has peaks in its visible spectrum at 562 and 676 nm. The infrared spectrum contains two peaks at 2021 and 1973 cm^{-1}, which indicates that this product contains terminal carbonyl ligands. The formula of $[Ir_3(\mu\text{-}H)(CO)_3(\eta^5\text{-}C_9H_7)_3][BF_4]$ (**2**) is supported by elemental analysis and the mass spectrum of the isolated purple solid.

The ^{1}H NMR spectrum of **2** contains a single hydride resonance at δ −19.1 and exhibits two sets of indenyl resonances in a 2:1 ratio. The pattern for the smaller set indicates that the indenyl ligand resides in a symmetric environment. Furthermore, the ^{13}C NMR spectrum of a ^{13}CO-enriched sample of **2** contains two peaks in the carbonyl region at δ 168.6 and 175.8 in a 2:1 ratio, respectively. These spectroscopic data are consistent with C_s geometry for **2**, with a mirror plane that is perpendicular to the Ir_3 plane and passes through one iridium atom (and its indenyl ligand) as well as the proton bridging the midpoint between the two remaining iridium atoms (see Scheme 1).

In comparison, we previously reported that the reactions of **1** with Cu^+, Ag^+, Au^+, and Hg^{2+} fragment electrophiles generate cationic tetranuclear butterfly clusters with the electrophile bridging one Ir−Ir edge.[6] The solid-state structure of one of these adducts, $[Ir_3\{Au(PPh_3)\}(CO)_3(\eta^5\text{-}C_9H_7)_3][PF_6]$, indicated the $Ir_3(CO)_3L_3$ substructure had rearranged to a C_s geom-

(1) Wadepohl, H.; Gebert, S. *Coord. Chem. Rev.* **1995**, *143*, 535.
(2) Barnes, C. E. In *Comprehensive Organometallic Chemistry II*; Abel, E. W., Stone, F. G. A., Wilkinson, G., Eds.; Pergamon: New York, 1995; Vol. 8, Chapter 4.
(3) Braga, D.; Grepioni, F.; Wadepohl, H.; Gebert, S.; Calhorda, M. J.; Veiros, L. F. *Organometallics* **1995**, *14*, 5350.
(4) (a) Robben, M. P.; Rieger, P. H.; Geiger, W. E. *J. Am. Chem. Soc.* **1999**, *121*, 367. (b) Robben, M. P.; Geiger, W. E.; Rheingold, A. L. *Inorg. Chem.* **1994**, *33*, 5615.
(5) Comstock, M. C.; Wilson, S. R.; Shapley, J. R. *Organometallics* **1994**, *13*, 3805.
(6) Comstock, M. C.; Prussak-Wieckowska, T.; Wilson, S. R.; Shapley, J. R. *Organometallics* **1997**, *16*, 4033.

10.1021/om020863w CCC: $22.00
Publication on Web 11/27/2002

Scheme 1

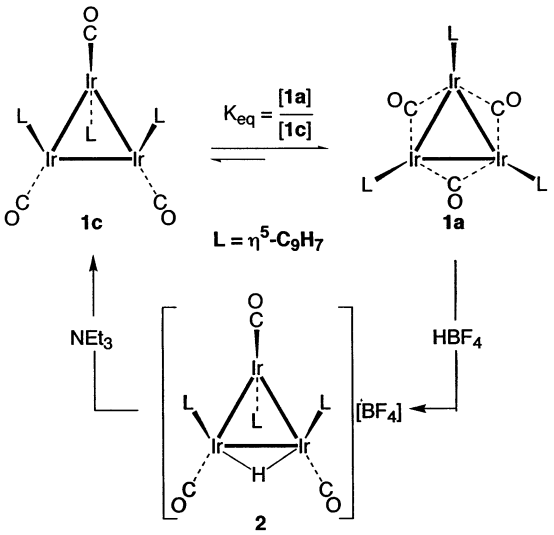

etry, differing from the C_{3v} symmetry observed for the parent cluster $Ir_3(CO)_3(\eta^5\text{-}C_9H_7)_3$ (**1**) in the solid state.[5] It is often observed that coinage-metal fragments occupy the same position as H^+ in the analogous protonated clusters,[7] and therefore it is likely that **2** has a solution structure very similar to the solid-state structure of $[Ir_3\{Au(PPh_3)\}(CO)_3(\eta^5\text{-}C_9H_7)_3][PF_6]$. This suggestion is further supported by the fact that deprotonation leads to a compound with C_s symmetry, **1c**.

Deprotonation of $[Ir_3(\mu\text{-}H)(CO)_3(\eta^5\text{-}C_9H_7)_3][BF_4]$. Addition of triethylamine to a purple solution of **2** in dichloromethane at room temperature leads immediately to an emerald green solution of isomer **1c** (see Scheme 1). The visible spectrum of this solution has peaks at 610 and 780 nm. The infrared spectrum, with peaks at 1967 and 1931 cm^{-1}, indicates the carbonyl ligands are bound in a terminal fashion. The proton NMR of **1c** at −80 °C is similar to that for **2**; two sets of indenyl resonances in a 2:1 ratio are observed, with the smaller set indicating that the indenyl ligand resides in a symmetric environment. Similarly, the ^{13}C NMR spectrum of a ^{13}CO-enriched sample of **1c** at −70 °C contains two peaks at δ 178.7 and 180.9 in a 2:1 ratio, respectively. For comparison, the structurally characterized cyclopentadienyl analogue $C_s\text{-}Ir_3(CO)_3(\eta^5\text{-}C_5H_5)_3$ shows IR peaks at 1960 and 1918 cm^{-1} (in CH_2Cl_2), and its ^{13}C NMR spectrum has carbonyl signals at 178.2 and 179.9 ppm in a 2:1 ratio.[8] At room temperature the green color of a solution of **1c** is replaced within minutes by the red color observed for a solution of **1**.

Equilibrium between the C_{3v} and C_s Isomers of $Ir_3(CO)_3(\eta^5\text{-}C_9H_7)_3$. The crystalline form of compound **1** previously isolated is now designated as the C_{3v} isomer (**1a**).[5] Dissolving these crystals in CH_2Cl_2 forms a spectroscopically pure solution of **1a**; the infrared spectrum shows only peaks at 1808 and 1763 cm^{-1}, and the maximum absorption in the visible spectrum appears at 562 nm. Within minutes, however, peaks due to **1c** appear. After approximately 15 min, the relative intensities of the peaks due to **1a** and **1c** remain constant, indicating that an equilibrium mixture **1a/1c** is established. The equilibrium constant, $K_{eq} = [\mathbf{1a}]/[\mathbf{1c}]$, was measured at different temperatures, and a plot of $\ln(K_{eq})$ vs $1/T$ provided the thermodynamic parameters $\Delta H° = -5.6(2)$ kcal mol^{-1} and $\Delta S° = -13.3(6)$ cal mol^{-1} K^{-1} (see Table 1).

Table 1. Kinetics and Thermodynamic Data for Interconversion of Isomers 1a and 1c

T, °C	k[a] ($\times 10^{-3}$ s^{-1})	K_{eq}([**1a**]/[**1c**])[b]
30	5.71(12)	15.0(7)
25	3.33(9)	16.7(7)
20	1.98(10)	19.8(9)
15	1.14(8)	23.7(10)
10	0.75(3)	27.9(10)

[a] Derived parameters: $\Delta H^{\ddagger} = 17.0(3)$ kcal mol^{-1}; $\Delta S^{\ddagger} = -13(1)$ cal mol^{-1} K^{-1}. [b] Derived parameters: $\Delta H^{o} = -5.6(2)$ kcal mol^{-1}; $\Delta S^{o} = -13.3(6)$ cal $mol^{-1}K^{-1}$.

Chart 2

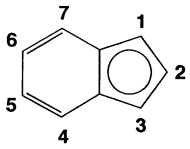

The kinetics of the conversion from **1c** to the equilibrium mixture **1a/1c** have been examined by observing the decrease in intensity of the peak at 780 nm in the electronic spectrum of **1c**. Rate constants were calculated from the slopes of plots of $\ln[(A_{eq} - A_t)/(A_{eq} - A_0)]$ vs time. The activation parameters, determined from Eyring plots of $\ln(k/T)$ vs $1/T$, were $\Delta H^{\ddagger} = 17.0(3)$ kcal mol^{-1} and $\Delta S^{\ddagger} = -13(1)$ cal mol^{-1} K^{-1} (see Table 1).

Fluxional Behavior of Isomer 1c. The ^1H NMR spectrum at −80 °C and the ^{13}C NMR spectrum at −70 °C of **1c** are consistent with C_s symmetry as described above. However, as the sample temperature increases toward 0 °C, the two unique sets of indenyl resonances for **1c** (H_1 and H_3; see Chart 2) broaden and then coalesce. Coalescence occurs at $T_c = -30$ °C, leading to the estimate (with $\Delta\nu = 18$ Hz) of $\Delta G_c^{\ddagger} = 12.4(3)$ kcal mol^{-1}. Over the same temperature range, however, the two carbonyl ligand signals (2:1 ratio) seen in the ^{13}C NMR spectrum of **1c** remain invariant in both the peak intensity and line width.

This fluxional behavior of isomer **1c** is readily rationalized by proposing an intermediate of structure B that is produced by pairwise bridging of terminal carbonyls on opposite faces of the Ir_3 triangle (see Scheme 2). The plane of symmetry in intermediate **1b** relates two previously distinct indenyl ligands (L_1, L_2) but does not change the relationship among carbonyl ligands a, b, and c. This highly precedented process was invoked to explain rapid carbonyl ligand scrambling in the C_s isomer of $Rh_3(CO)_3(\eta^5\text{-}C_5H_5)_3$,[9] which had been crystallographically characterized.[10] Furthermore, two recent theoretical studies of $M_3(CO)_3L_3$ compounds agree on the relatively close energies of structures B and C for

(7) (a) Salter, I. D. In *Comprehensive Organometallic Chemistry II*; Abel, E. W., Stone, F. G. A., Wilkinson, G., Eds.; Pergamon: New York, 1995; Vol. 10, Chapter 5. (b) Salter, I. D. *Adv. Organomet. Chem.* **1989**, *29*, 249.

(8) Shapley, J. R.; Adair, P. C.; Lawson, R. J.; Pierpont, C. G. *Inorg. Chem.* **1982**, *21*, 1701.

(9) (a) Lawson, R. J.; Shapley, J. R. *J. Am. Chem. Soc.* **1976**, *98*, 7433. (b) Lawson, R. J.; Shapley, J. R. *Inorg. Chem.* **1978**, *17*, 772.

(10) (a) Paulus, E. F. *Acta Crystallogr., Sect. B* **1969**, *25*, 2206. (b) Paulus, E. F.; Fischer, E. O.; Fritz, H. P.; Schuster-Woldan, H. *J. Organomet. Chem.* **1967**, *10*, P3. (c) Mills, O. S.; Paulus, E. F. *J. Organomet. Chem.* **1967**, *10*, 331.

Scheme 2

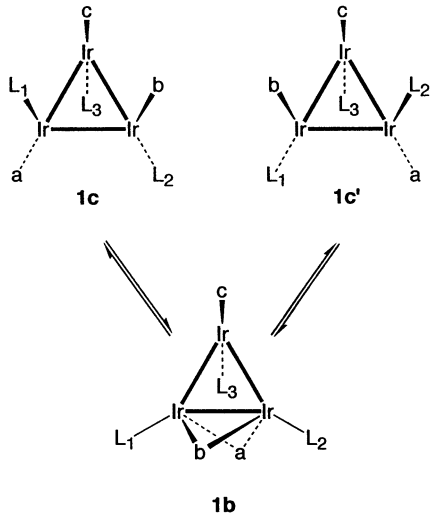

Scheme 3

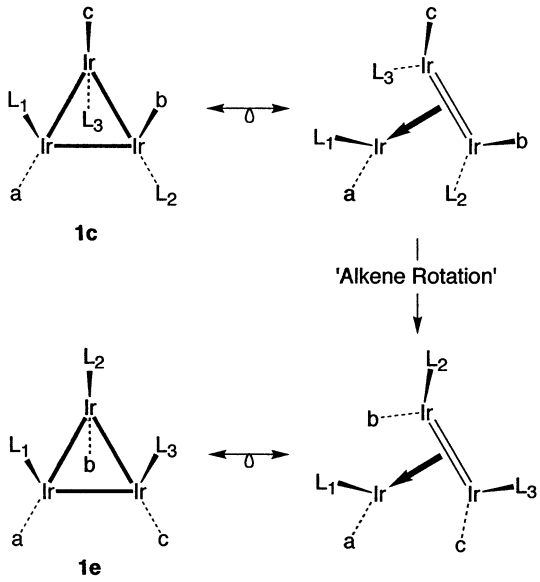

triiridium compounds.[3,11] Although the details are not as well defined, the cyclopentadienyl analogue C_s-$Ir_3(CO)_3(\eta^5\text{-}C_5H_5)_3$ appears also to undergo a similar equilibration of the Cp groups—but not the carbonyl ligands—over a comparable temperature range.[12]

Interconversion of 1c and 1a. The conversion of triply edge-bridged structure A with any one of the structures B, C, or D requires moving one carbonyl ligand across the M_3 triangle edge from one face to the other. The barrier for A to B isomerization in the case of $Co_3(CO)_3(\eta^5\text{-}C_5H_5)_3$ has been estimated by a molecular mechanics method as 16.5 kcal/mol, and this was regarded as a lower bound.[11] The reverse conversion of type B to type A structures requires heating at elevated temperatures in the cases of $Rh_3(CO)_3(\eta^5\text{-}C_5H_5)_3$[9] and $IrCo_2(CO)_3(\eta^5\text{-}C_5Me_5)(\eta^5\text{-}C_5H_5)_2$.[13] In the case of the $IrCo_2$ compound both the rate of approach to equilibrium and its position were determined at various temperatures.[13] The derived thermodynamic parameters for the equilibrium (K_{eq} = [A]/[B]), $\Delta H° = -6.5$ kcal mol^{-1} and $\Delta S° = -17.8$ cal mol^{-1} K^{-1}, are rather similar to those presented here (K_{eq} = [**1a**]/[**1c**]; see Table 1). In both cases the A configuration is favored by enthalpy but significantly disfavored by entropy, perhaps due to solvent ordering around the more polar structure. However, the reported kinetic parameters for the $IrCo_2$ compound, $\Delta H^‡ = 107(4)$ kJ/mol (25.6 kcal mol^{-1}) and $\Delta S^‡ = 2(11)$ J mol^{-1} K^{-1} (0.5 cal mol^{-1} K^{-1}), are markedly different from those of our Ir_3 compound. The overall kinetic barrier is significantly higher ($\Delta G^‡(298) = 25.7$ kcal mol^{-1} for the $IrCo_2$ case vs. $\Delta G^‡(298) = 20.9$ kcal mol^{-1} for the Ir_3 case), consistent with the 1000-fold faster isomerization rate at room temperature for the indenyl–iridium trimer. Thus, the interconversion of all-terminal form **1c** with all-bridged form **1a** not only is unique to this case but is also remarkably facile.

An explanation for the relatively facile isomerization relating **1c** and **1a** may be related to the "indenyl ligand effect" on the barrier to rotation about an M–alkene bond (M = Rh, Ir).[14] For example, the rotation barrier about the Ir–ethylene bond in the cyclopentadienyl compound $Ir(CO)(C_2H_4)(\eta^5\text{-}C_5H_5)$ is $\Delta G^‡(417) = 20.0$ kcal mol^{-1}, but this barrier is reduced to $\Delta G^‡(296) = 13.9$ kcal mol^{-1} in the corresponding indenyl compound $Ir(CO)(C_2H_4)(\eta^5\text{-}C_9H_7)$.[14a] The reduction is attributed to easier η^5-to-η^3 "slippage" for the benzo-fused indenyl ring that reduces a repulsive bonding interaction in the transition state.[14c] The structure of C_s-$Ir_3(CO)_3(\eta^5\text{-}C_5H_5)_3$ has been described as a pseudo-ethylene complex of $Ir(CO)(\eta^5\text{-}C_5H_5)$, incorporating a formally unsaturated $Ir_2(CO)_2(\eta^5\text{-}C_5H_5)_2$ moiety.[8] In fact, schemes involving addition of metal fragments to unsaturated dinuclear species isolobal with ethylene, such as $M_2(CO)_2(\eta^5\text{-}C_5Me_5)_2$ (M = Co, Rh) and $Re_2(\mu\text{-}H)_2(CO)_8$, are common in the synthesis of trinuclear clusters.[15] Furthermore, the barrier to rotation of the M═M unit about the axis connecting its midpoint to the third metal center can be similar to that for ethylene rotation.[16] These observations provide a precedent for the isomerization mechanism illustrated in Scheme 3. "Alkene rotation" of the *cis*-$Ir_2(CO)_2(\eta^5\text{-}C_9H_7)_2$ unit in **1c** results in the formation of the all-terminal carbonyl form **1e**, which can readily close to the triply bridged structure observed for C_{3v}-$Ir_3(\mu\text{-}CO)_3(\eta^5\text{-}C_9H_7)_3$ (**1a**). Molecular mechanics calculations on the various possible forms of $Ir_3(\mu\text{-}CO)_3(\eta^5\text{-}C_9H_7)_3$ placed the relative energy of **1c** vs **1a** at 6.0 kcal/mol,[11] remarkably close to the experimental enthalpy difference. On the same scale the C_{3v}-symmetric, all-terminal form **1e** had a calculated energy of 9.8 kcal/mol, the highest of all the configurations. Nevertheless, these energy differences are certainly

(11) Mercandelli, P.; Sironi, A. *J. Am. Chem. Soc.* **1996**, *118*, 11548.
(12) Adair, P. C. Ph.D. Thesis. University of Illinois, 1980.
(13) Geiger, W. E.; Shaw, M. J.; Wünsch, M.; Barnes, C. E.; Foersterling, F. H. *J. Am. Chem. Soc.* **1997**, *119*, 2804.

(14) (a) Szajek, L. P.; Lawson, R. J.; Shapley, J. R. *Organometallics* **1991**, *10*, 357. (b) Eshtiagh-Hosseini, H.; Nixon, J. F. *J. Less-Common Met.* **1978**, *61*, 107. (c) Mlekuz, M.; Bougeard, P.; Sayer, B. G.; McGlinchey, M. J.; Rodgers, C. A.; Churchill, J. W.; Zeller, J.; Kans, S.-W.; Albright, T. A. *Organometallics* **1986**, *5*, 1656. (d) Kakkar, A. K.; Taylor, N. J.; Calabrese, J. C.; Nugent, W. A.; Roe, D. C.; Connaway, E. A.; Marder, T. B. *J. Chem. Soc., Chem. Commun.* **1989**, 990.
(15) (a) Comstock, M. C.; Prussak-Wieckowska, T.; Wilson, S. R.; Shapley, J. R. *Inorg. Chem.* **1997**, *36*, 4397 and references therein. (b) Stone, F. G. A. *Angew. Chem., Int. Ed. Engl.* **1984**, *23*, 89.
(16) (a) Barr, R. D.; Green, M.; Howard, J. A. K.; Marder, T. B.; Orpen, A. G.; Stone, F. G. A. *J. Chem. Soc., Dalton Trans.* **1984**, 2757. See also: (b) Cooke, J.; McClung, R. E. D.; Takats, J.; Rogers, R. D. *Organometallics* **1996**, *15*, 4459. (c) Beringhelli, T.; D'Alfonso, G.; Freni, M.; Panigati, M. *Organometallics* **1997**, *16*, 2719.

surmountable by thermal activation and would not preclude **1e** as a viable intermediate. An all-terminal form of type E is very likely accessible as an intermediate for the facile internuclear scrambling of carbonyl ligands occurring in C_{3v}-$Rh_3(CO)_3(\eta^5\text{-}C_5H_5)_3$.[9]

Finally, it is important to note that the isomerization rate between a type A structure and a type B or D structure is dramatically increased by one-electron oxidation or reduction, which has been attributed to loss of net metal−metal bonding in either the cation or anion.[13,17] This interpretation is also consistent with the facile isomerization induced by the addition of an electrophile to **1a**, either a proton (to form **2**) or a metal complex fragment,[6] since this interaction significantly weakens one of the metal−metal bonds.

Experimental Section

General Procedures. All synthetic preparations were conducted under an atmosphere of nitrogen by using standard Schlenk techniques. The cluster $Ir_3(CO)_3(\eta^5\text{-}C_9H_7)_3$ (**1**) was prepared as described previously.[5] The reagents $HBF_4{\cdot}Et_2O$ (85%, Aldrich) and NEt_3 (Fisher), as well as CD_2Cl_2 (Cambridge Isotope Laboratories), were used as received. Solvents for preparative use were dried by standard methods and distilled prior to use. The instrumentation and facilities used have been listed.[5]

$[Ir_3(\mu\text{-}H)(CO)_3(\eta^5\text{-}C_9H_7)_3][BF_4]$ (2). A dark red CH_2Cl_2 solution (5 mL) of **1** (51 mg, 0.051 mmol) was treated dropwise with $HBF_4{\cdot}Et_2O$ (85%) (10.7 μL, 0.056 mmol), resulting in an immediate color change to a deep purple. After the solvent was removed under vacuum, the residue was triturated with diethyl ether and then dried under vacuum to give a purple solid (44 mg, 0.040 mmol, 79%). IR (CH_2Cl_2): ν_{co} 2021, 1973 cm^{-1}. Anal. Calcd for $C_{30}H_{22}BF_4Ir_3O_3$: C, 32.94; H, 2.03. Found: C, 32.81; H, 2.08. UV−vis (CH_2Cl_2): λ_{max} (ϵ) 390 sh (8570), 450 (4920), 562 (6830), 676 (2330) nm. FAB-MS: *m*/*z* (^{193}Ir) 1006, $[Ir_3(CO)_3(C_9H_7)_3^+]$. ^{1}H NMR (300 MHz, CD_2Cl_2, 20 °C; see Chart 2 for key to assignments): δ 7.65−7.25 m (12 H, H_4−H_7, $L_1 + 2L_2$), 6.02 t (1H, H_2, L_1, $J_{12} = J_{13} = 2.6$ Hz), 5.98 d (2H, $H_1 + H_3$, L_1), 6.00 m + 5.89 m (2H + 2H, $H_1 + H_3$, $2L_2$), 5.78 m (2H, H_2, $2L_2$). ^{13}C NMR (125 MHz, CD_2Cl_2, 20 °C): δ 175.8 (1CO), 168.6 (2CO).

C_s-$Ir_3(CO)_3(\eta^5\text{-}C_9H_7)_3$ (1c). Addition of NEt_3 (1.4 μL, 1.0 mg, 0.010 mmol) to a purple CH_2Cl_2 solution (10 mL) of **2** (11 mg, 0.010 mmol) at room temperature resulted in the immediate formation of a green solution of C_s-$Ir_3(CO)_3(\eta^5\text{-}C_9H_7)_3$ (**1c**). However, this solution rapidly reverted to the equilibrium mixture **1a/1c** at 25 °C. Both infrared and UV−visible spectroscopic data were recorded by acquiring data immediately after generation of **1c**. IR (CH_2Cl_2): ν_{CO} 1967, 1931 cm^{-1}. UV−vis (CH_2Cl_2): λ_{max} (ϵ) 368 sh (12 040), 424 sh (9270), 610 (4610), 780 (2274) nm. ^{1}H NMR (300 MHz, CD_2Cl_2, −80 °C; see Chart 2 for key to assignments): δ 7.45−6.94 m (12 H, H_4−H_7, $L_1 + 2L_2$), 5.72 m + 5.66 m (2H + 2H, $H_1 + H_3$, $2L_2$), 5.58 d (2H, $H_1 + H_3$, L_1), 5.08 t (1H, H_2, L_1, $J_{12} = J_{13} = 2.6$ Hz), 4.63 m (2H, H_2, $2L_2$). ^{13}C NMR (125 MHz, CD_2Cl_2, −70 °C): δ 180.9 (1CO), 178.7 (2CO).

Kinetics and Equilibrium. Solutions of isomer **1c** in CH_2Cl_2 were generated as described above with the initial concentration of **1c** = 3.33×10^{-4} M. The decrease in the intensity of the absorbance at 780 nm was monitored as the system returned to equilibrium. Plots of $\ln[(A_{eq} - A_t)/(A_{eq} - A_0)]$ vs time (where A_{eq} = the absorbance at equilibrium) were linear over at least 2−3 half-lives. Activation parameters were derived from a plot of $\ln(k/T)$ vs $1/T$. Errors in $\Delta H^{\ddagger}$ and $\Delta S^{\ddagger}$ were the standard deviations about the average values derived from four replicate experiments. The equilibrium constant, K_{eq} = [**1a**]/[**1c**], for a 1.42×10^{-3} M solution of **1a/1c** in CH_2Cl_2, was measured at different temperatures, where [**1c**] was determined by measuring the absorbance at 780 nm and [**1a**] was calculated assuming the concentration of [**1a**] = [**1a/1c**] − [**1c**]. Errors in K_{eq} were propagated from the error in the extinction coefficient of the peak at 780 nm. Thermodynamic parameters were obtained from a plot of $\ln(K_{eq})$ vs $1/T$. Errors in $\Delta H°$ and $\Delta S°$ were calculated from the standard errors in the slope and intercept obtained by the least-squares method.

Variable-Temperature NMR. A CD_2Cl_2 solution of **1** in an NMR tube was treated with 1 equiv of $HBF_4{\cdot}Et_2O$ to give **2**. The sample tube was cooled to 0 °C, and then 5 equiv of NEt_3 was added to form a solution of **1c**. The sample tube was then transferred to the precooled NMR probe. The free energy of activation, $\Delta G^{\ddagger}$, for the process causing equilibration of the indenyl ligands was calculated from the rate constant at the temperature of coalescence of the indenyl H_2 protons by using the equations $k_c = \pi(\Delta\nu)2^{-1/2} = (k_b T_c/h)\exp[-\Delta G_c^{\ddagger}/RT_c]$. The error in $\Delta G_c^{\ddagger}$ was propagated from the estimated error in T_c.

Acknowledgment. This research was supported in part by a grant from the National Science Foundation. M.C.C. thanks the Department of Chemistry for a fellowship funded by the Lubrizol Corp.

OM020863W

(17) Robben, M. P.; Rieger, P. H.; Geiger, W. E. *J. Am. Chem. Soc.* **1999**, *121*, 367.